

Event-Anchored Frame Selection for Effective Long-Video Understanding

Wang Chen^{1*}, Yongdong Luo^{1*}, Yuhui Zeng¹, Luojun Lin²,
Tianyu Xie¹, Fei Chao¹, Rongrong Ji¹, Xiawu Zheng^{1†}

¹Key Laboratory of Multimedia Trusted Perception and Efficient Computing,
Ministry of Education of China, Xiamen University

²College of Computer and Data Science, Fuzhou University

Abstract

Massive frame redundancy and limited context window make efficient frame selection crucial for long-video understanding with large vision-language models (LVLMs). Prevailing approaches, however, adopt a flat sampling paradigm which treats the video as an unstructured collection of frames. In this paper, we introduce **Event-Anchored Frame Selection (EFS)**, a hierarchical, event-aware pipeline. Leveraging self-supervised DINO embeddings, EFS first partitions the video stream into visually homogeneous temporal segments, which serve as proxies for semantic events. Within each event, it then selects the most query-relevant frame as an anchor. These anchors act as structural priors that guide a global refinement stage using an adaptive Maximal Marginal Relevance (MMR) scheme. This pipeline ensures the final keyframe set jointly optimizes for event coverage, query relevance, and visual diversity. As a **training-free, plug-and-play module**, EFS can be seamlessly integrated into off-the-shelf LVLMs, yielding substantial gains on challenging video understanding benchmarks. Specifically, when applied to LLaVA-Video-7B, EFS improves accuracy by **4.7%**, **4.9%**, and **8.8%** on VideoMME, LongVideoBench, and MLVU, respectively.

1. Introduction

The remarkable success of Large Language Models (LLMs) in natural language processing [1] has catalyzed their extension into multimodal domains. By integrating powerful visual encoders with advanced reasoning capabilities of LLMs, Large Vision-Language Models (LVLMs) [15, 36] have emerged, rapidly advancing machine perception. Leveraging pre-training on large-scale video-text datasets, LVLMs are now capable of complex video tasks such as detailed video captioning [5], nuanced question answer-

Query: Which of the following options correctly sorts the events of the following heroines in chronological order?

① Study ② Make the bed ③ Eat breakfast ④ Exercise at home

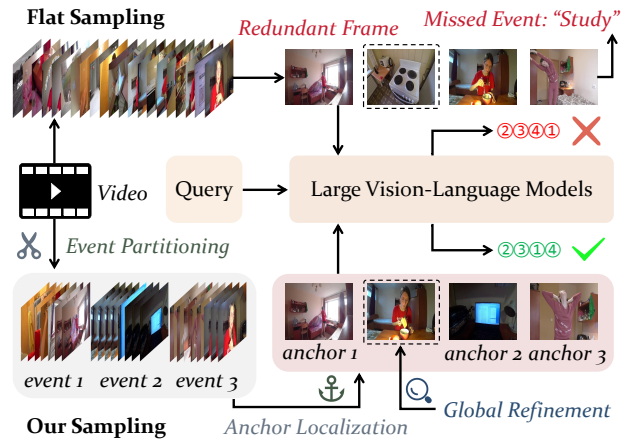


Figure 1. A conceptual illustration of our Event-anchored Frame Selection (EFS) in contrast to the flat sampling baseline. Flat sampling often yields redundant frames and misses key events, causing LVLMs to fail, while EFS partitions videos into events, selects query-relevant anchors, and performs anchor-guided global refinement to enable correct chronological reasoning.

ing [23], and sophisticated temporal reasoning [29].

Despite these successes, LVLMs confront a fundamental bottleneck with long-form videos: the massive number of frames clashes with limited computational budget and fixed context windows. Directly processing every frame is simply infeasible. This necessitates a mechanism to condense the vast visual stream into a concise yet representative input. Consequently, frame selection has become a critical, pragmatic prerequisite for applying LVLMs to real-world long-form content. While alternative strategies like extending context windows [16, 42] or video-to-text summarization [21] exist, they often incur prohibitive computational overhead or significant information loss, making efficient frame selection a more direct and balanced approach.

*Equal contribution.

†Corresponding author.

However, the effectiveness of frame selection depends entirely on how frames are selected. Many existing techniques [8, 10, 28, 34, 38–40, 43] utilize a flat sampling paradigm, treating the video as an unstructured collection of frames and disregarding higher-level semantic relationships. This paradigm is fundamentally temporally-agnostic, overlooking the intrinsic narrative and event structure of video. Consequently, these methods often fail to select a frame set that simultaneously and effectively balances the three essential pillars of ideal selection: query relevance, comprehensive event coverage, and sufficient visual diversity. As illustrated in Figure 1, a flat sampling strategy is prone to missing crucial events, leading LVLMs to reach incorrect conclusions.

To overcome this limitation, we propose shifting from a temporally-agnostic to an event-aware perspective. We introduce Event-Anchored Frame Selection (EFS), a hierarchical, training-free pipeline grounded in the intrinsic event structure of video. Our core insight is that an optimal keyframe set must be built upon a macroscopic understanding of the narrative flow of video. EFS first partitions the video into visually coherent temporal segments, serving as reliable proxies for semantic events. It then establishes a structural “backbone” by selecting the most query-relevant frame from each event as an anchor. This initial set of event anchors then guides a global refinement stage, which leverages an adaptive Maximal Marginal Relevance (MMR) scheme to enrich the selection with diverse, informative frames. This hierarchical process ensures the final keyframe set jointly optimizes for event coverage, query relevance, and visual diversity.

As a plug-and-play module, EFS can be seamlessly integrated with off-the-shelf LVLMs without any additional training. We validate EFS on three widely used long-video question-answering benchmarks: VideoMME [9], LongVideoBench [37], and MLVU [45]. Across all benchmarks, EFS delivers consistent and substantial performance gains. Specifically, when applied to LLaVA-Video-7B and LLaVA-OneVision-7B, EFS improves accuracy by **4.7%**, **4.9%**, and **8.8%**, and by **3.3%**, **6.2%**, and **8.8%** on VideoMME, LongVideoBench, and MLVU, respectively. These results demonstrate that event-aware frame selection is essential for unlocking the full potential of LVLMs in long-video understanding.

Our main contributions can be summarized as follows:

- We propose Event-Anchored Frame Selection (EFS), a training-free hierarchical framework that perceives a macroscopic event structure of video before performing fine-grained frame selection, surpassing the limitations of flat, temporally-agnostic sampling.
- We design an anchor-guided global refinement strategy that employs an adaptive MMR scheme. This method dynamically calibrates the diversity threshold based on the

video’s own content statistics, enhancing robustness and adaptability across different video types.

- We conduct extensive experiments on three challenging long-video understanding benchmarks and demonstrate that EFS significantly boosts the reasoning performance of existing LVLMs, clearly underscoring the value of event-aware frame selection.

2. Related Work

LVLMs for Long Video Understanding. Despite impressive performance on short clips [14, 22], LVLMs face significant challenges with long-form videos due to massive frame redundancy and limited context windows. To mitigate this, one line of research focuses on architectural modifications, such as extending the context window for the model [16, 42] or reducing visual tokens by pruning and merging [13, 20, 32]. However, these approaches often suffer from high computational overhead or risk discarding critical visual details. Another strategy involves converting video content into text to leverage the language capabilities of LLMs [7, 19, 21, 28]. This method, while efficient, still leads to significant information loss, constraining the understanding of visual nuances.

Frame Selection for Video Understanding. Frame selection provides a practical alternative to the approaches above. Traditional methods like uniform sampling or early keyframe extraction [24, 31] are often query-agnostic and insufficient for complex reasoning tasks. Recent work explores query-based frame selection, ranking frames by relevance to specific queries. For example, BOLT [17] applies inverse transform sampling, while Frame-Voyager [40] uses a ranking-based pipeline for optimal frame combinations. Other notable methods include mDP³ [34], which formulates frame selection as a Markov decision process combined with determinantal point processes, AKS [35], which jointly optimizes for both query relevance and video coverage, Q-frame [43], which processes frames with dynamic resolutions, KFC [8], which models the problem as subgraph selection, and T* [39], which applies an temporal object-centric search. Although these methods can improve query relevance or diversity, they predominantly adopt a flat sampling paradigm, treating video as an unstructured frame sequence and ignoring event structure, which limits event coverage. In contrast, our hierarchical event-aware framework jointly optimizes relevance, coverage, and diversity.

3. Methodology

In this section, we elaborate on our Event-Anchored Frame Selection framework. As illustrated in Figure 2, EFS first obtains a macroscopic understanding by partitioning the video into coherent visual events. This events structure then guides a global refinement process to produce a keyframe

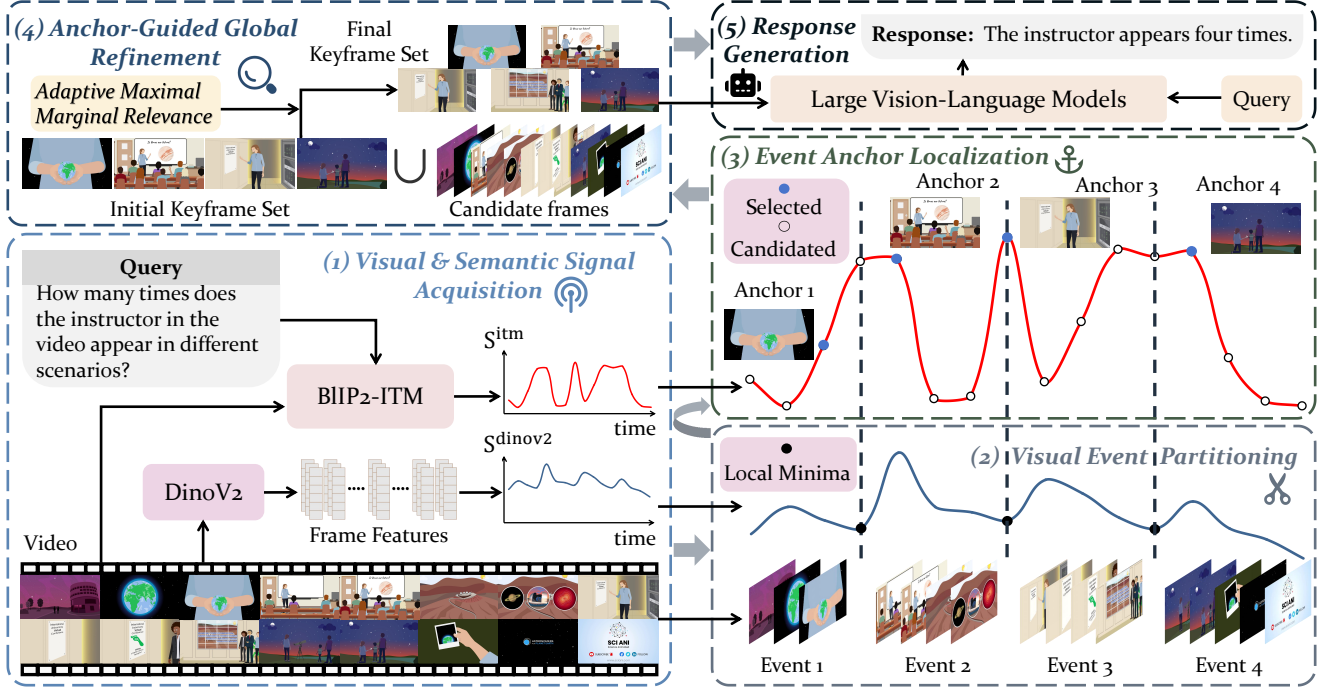


Figure 2. An illustration of our Event-Anchored Frame Selection (EFS) pipeline. Given a user query, such as “How many times does the instructor appear in different scenarios?”, EFS operates in distinct stages: (1) It first acquires visual signals (from DinoV2) and semantic relevance scores (from BLIP2-ITM). (2) The visual signals are used to partition the video into coherent events at local minima of temporal similarity. (3) Within each event, it localizes the most query-relevant frame as an anchor. (4) This initial set of anchors is then globally refined via Adaptive MMR to form the final keyframe set. (5) Finally, this curated set enables the Large Vision-Language Models to accurately answer the query, correctly identifying the four appearances.

set optimized for relevance, coverage, and diversity.

3.1. Problem Formulation

Given a long video of T frames, $V = \{I_1, I_2, \dots, I_T\}$, and a user query Q , the task of keyframe selection is to extract a concise yet representative subset of frames $K = \{I_{t_1}, I_{t_2}, \dots, I_{t_k}\}$, where the indices are chronologically ordered and $k \ll T$. The value of k is typically pre-defined based on both the context window limitations of LVLMs and the requirements of downstream tasks or user preferences. The objective is to select K so that, when it is provided as visual context along with the query Q , an LVLm can generate the most accurate and comprehensive answer possible. This requires balancing three core objectives: ensuring thorough coverage of key events, maintaining strong relevance to the query, and promoting sufficient diversity to minimize redundancy.

However, the most strategy in existing LVLm-based long-video understanding pipelines is uniform sampling. While simple and efficient, it largely disregards the intrinsic temporal and semantic structure of the video, often missing critical, query-relevant events and introducing redundant or uninformative frames. Hence, more intelligent, structure-

aware keyframe selection frameworks are needed.

3.2. Visual & Semantic Signal Acquisition

We begin by sampling the video at 1 frame-per-second, yielding a length- N candidate frame sequence $\mathcal{I} = \{I_1, I_2, \dots, I_N\}$. In this sequence, we extract two fundamental signals for each frame.

Image-Text Matching. To quantify the semantic relevance of each frame to the query, we use the Image-Text Matching (ITM) head of Blip2 [12] (referred to as BLIP2-ITM), which is designed to output a score indicating the alignment between a given image and a text description. This score serves as an excellent measure of query relevance. For each frame I_i and the text query Q , the relevance score is computed as:

$$s_i^{\text{itm}} = \text{BLIP2-ITM}(I_i, Q), \quad (1)$$

These scores, forming a relevance signal $\{s_1^{\text{itm}}, \dots, s_N^{\text{itm}}\}$, which in turn allows us to prioritize frames that pertain to the user’s specific information need.

Temporal Similarity Calculation. To understanding the temporal structure of the video, we measure visual similarity between frames using DINOv2 [27], a powerful self-supervised model known for its robust visual embeddings

that capture both high-level semantic content and low-level structural details without requiring explicit labels. Its features are particularly effective at discerning meaningful changes in visual content. For each frame I_i , we extract its DINOv2 feature vector, $\mathbf{f}_i \in \mathbb{R}^d$, and L2-normalize it. Using these embeddings, we then compute an inter-frame temporal similarity score, $s_i^{\text{dino}v2}$, for each frame i by comparing it to its neighbors within a weighted sliding window of size l . This captures the local visual coherence:

$$s_i^{\text{dino}v2} = \frac{\sum_{j \in \mathcal{N}(i)} w_{|i-j|} \cdot \cos(\mathbf{f}_i, \mathbf{f}_j)}{\sum_{j \in \mathcal{N}(i)} w_{|i-j|}}, \quad (2)$$

where $\mathcal{N}(i)$ is the neighborhood of frame i , and the weight w_d decreases linearly as the distance $d = |i - j|$ increases. Based on empirical design, we set l to 3; detailed ablation studies can be found in the Appendix. The resulting inter-frame temporal similarity curve, $\{s_1^{\text{dino}v2}, \dots, s_N^{\text{dino}v2}\}$, reveals the rhythm of visual changes throughout the video.

3.3. Event-Anchored Frame Selection

Our EFS method follows a three-stage, coarse-to-fine process: partitioning the video into events, localizing an anchor in each event, and performing a globally-aware refinement. **Visual Event Partitioning.** We conceptualize “events” as visually homogeneous temporal segments. In video production, a significant change in visual content—such as a camera cut or a major shift in scenery—typically marks the boundary between distinct scenes or events. These moments directly correspond to local minima in our temporal similarity curve $\{s_1^{\text{dino}v2}, \dots, s_N^{\text{dino}v2}\}$, as they signify maximum visual change. Directly selecting these minima as our initial event boundaries is highly efficient and incurs no extra overhead, unlike approaches that rely on clustering or other computationally intensive segmentation methods.

However, long videos often contain hundreds of events, exceeding the practical token budget of LVLMS. To address this, we set a target event count M . If the initial partitioning yields more than M events, we iteratively merge the most similar adjacent pair, using the cosine similarity between their mean DINOv2 features. This continues until exactly M visually distinct, temporally coherent events $\{\mathcal{G}_1, \mathcal{G}_2, \dots, \mathcal{G}_M\}$ remain, forming the macroscopic structural for our selection.

Event Anchor Localization & Initialization. To ensure both complete event coverage and strong query alignment, we initialize our keyframe set by selecting one representative frame from each event. Given the importance of the user query in video understanding tasks, we select the frame with the highest query-relevance score s_i^{itm} within each event \mathcal{G}_j to serve as its “anchor”. This can be formulated as

$$k_j^{\text{anchor}} = \arg \max_{i \in \mathcal{G}_j} s_i^{\text{itm}}, \quad (3)$$

This set of anchors, $\mathcal{K}_{\text{init}} = \{k_1^{\text{anchor}}, \dots, k_M^{\text{anchor}}\}$, forms an initial keyframe set that is firmly grounded in the video’s event structure while being centered on the query’s focus.

Algorithm 1 Anchor-Guided Global Refinement

```

1: Input: Candidate frames  $\mathcal{C}$ , Anchor set  $\mathcal{K}_{\text{init}}$ , DINOv2
   frame features  $\mathbf{f}$ , Relevance scores  $s_i^{\text{itm}}$ , Target size  $k$ ,
   Threshold relaxation factor  $\alpha$ , Increment  $\delta$ .
2: Output: Final keyframe set  $\mathcal{K}$ .
3:  $\mathcal{K} \leftarrow \mathcal{K}_{\text{init}}$ ; Sort  $\mathcal{C}$  descending by relevance score  $s_i^{\text{itm}}$ .
4:  $\mu, \sigma \leftarrow \text{mean, std}(\{\max_{I_j \in \mathcal{K}_{\text{init}}} \cos(\mathbf{f}_i, \mathbf{f}_j) \mid I_i \in \mathcal{C}\})$ 
   // Estimate similarity distribution of  $\mathcal{C}$  to  $\mathcal{K}_{\text{init}}$ .
5:  $\theta_{\text{strict}}, \theta_{\text{loose}} \leftarrow \text{clip}(\mu - \alpha\sigma, 0, 1), \text{clip}(\mu + \alpha\sigma, 0, 1)$ 
   // Set adaptive strict and loose thresholds.
6:  $\theta_{\text{current}} \leftarrow \theta_{\text{strict}}$ 
7: while  $|\mathcal{K}| < k$  and  $\theta_{\text{current}} \leq \theta_{\text{loose}}$  do
8:   for  $I_c$  in  $\mathcal{C} \setminus \mathcal{K}$  do
9:     if  $|\mathcal{K}| \geq k$  then break
10:    end if
11:    if  $\max_{I_j \in \mathcal{K}} \cos(\mathbf{f}_c, \mathbf{f}_j) < \theta_{\text{current}}$  then
12:       $\mathcal{K} \leftarrow \mathcal{K} \cup \{I_c\}$ 
      // Add frame if below current threshold.
13:    end if
14:  end for
15:   $\theta_{\text{current}} \leftarrow \min(\theta_{\text{current}} + \delta, \theta_{\text{loose}})$ 
   // Relax threshold for next round.
16: end while
17: return  $\mathcal{K}$ 

```

Anchor-Guided Global Refinement. The anchor set provides a strong but sparse representation. The final step is to refine this set by adding more frames to enhance detail and diversity. A classic approach for this is Maximal Marginal Relevance (MMR) [3], which aims to select items that are both relevant to a query and dissimilar to already selected items:

$$\arg \max_{I_i \in \mathcal{C}} \left[\lambda \cdot \text{sim}(I_i, Q) - (1 - \lambda) \max_{I_j \in \mathcal{K}} \text{sim}(I_i, I_j) \right]. \quad (4)$$

Here, \mathcal{K} denotes the set of selected frames, \mathcal{C} refers to the remaining frames, and hyperparameter λ balances relevance and diversity. This method rescores all candidates at each step, resulting in a computational complexity of about $\mathcal{O}(|\mathcal{C}||\mathcal{K}|^2)$, which can be demanding. To improve efficiency, [6] propose an approximate greedy algorithm that sort candidates by relevance and applying a fixed diversity threshold. However, this approach is not robust: a single threshold cannot adapt to varying visual pacing—what works for an action film may fail for a slow documentary.

Our central motivation is to make the diversity threshold adaptive and data-driven, guided by the intrinsic visual structure of each video. By leveraging previously generated event anchors as a statistical prior, our anchor-guided refinement strategy tailors the selection criteria to the content

Table 1. Video-based question answering accuracy (%) of previous LVLMs on Video-MME [9], LongVideoBench [37] and MLVU [45]. Our EFS is applied to three off-the-shelf LVLMs. Frames and LLM indicate the number of video frames input to the LVLMs and the number of parameters in the LLM part, respectively.

| Model | Params | Frames | VideoMME (w.o. sub.) | | | | LongVideo Bench (val) | MLVU (m-avg) |
|------------------------------|-----------|----------------|----------------------|--------------------|--------------------|--------------------|-----------------------|--------------------|
| | | | Short | Medium | Long | Overall | | |
| <i>Proprietary LVLMs</i> | | | | | | | | |
| GPT-4o mini [25] | - | 250 | 72.5 | 63.1 | 58.6 | 64.8 | - | - |
| GPT-4o [26] | - | 384/256/0.5fps | 80.0 | 70.3 | 65.3 | 71.9 | 66.7 | 64.6 |
| <i>Open-Source LVLMs</i> | | | | | | | | |
| Video-LLaVA [14] | 7B | 8 | 45.3 | 38.0 | 36.2 | 39.9 | 39.1 | 47.3 |
| LongVA [42] | 7B | 128/256 | 61.1 | 50.4 | 46.2 | 52.6 | - | 56.3 |
| Video-XL [33] | 7B | 128/256 | 64.0 | 53.2 | 49.2 | 55.5 | 50.7 | 64.9 |
| Frame-Voyager [40] | 7B | 8 | 67.3 | 56.3 | 48.9 | 57.5 | - | 65.6 |
| LongVU [32] | 7B | 1fps | - | - | 59.5 | 60.6 | - | 65.4 |
| NVILA [18] | 8B | 256 | 75.7 | 62.2 | 54.9 | 64.2 | 57.7 | 70.1 |
| LLaVA-OneVision [11] | 7B | 8 | 65.2 | 52.0 | 45.0 | 54.1 | 54.1 | 58.6 |
| LLaVA-OneVision + EFS | 7B | 8 | 70.4 (+5.2) | 55.7 (+3.7) | 46.0 (+1.0) | 57.4 (+3.3) | 60.3 (+6.2) | 67.4 (+8.8) |
| Qwen2.5-VL [2] | 7B | 16 | 68.0 | 57.0 | 47.8 | 57.6 | 57.0 | 56.5 |
| Qwen2.5-VL + EFS | 7B | 16 | 70.2 (+2.2) | 59.1 (+2.1) | 50.8 (+3.0) | 60.0 (+2.4) | 60.5 (+3.5) | 66.0 (+9.5) |
| LLaVA-Video [44] | 7B | 64 | 76.4 | 63.1 | 54.2 | 64.6 | 58.8 | 68.1 |
| LLaVA-Video + EFS | 7B | 64 | 77.3 (+0.9) | 64.3 (+1.2) | 55.2 (+1.0) | 65.6 (+1.0) | 62.1 (+3.3) | 70.9 (+2.8) |

redundancy of the source video. This approach dynamically adjusts the diversity threshold so that visually dense segments are subjected to stricter deduplication, while sparser regions are treated more inclusively. Such content-aware adaptation enables robust and equitable keyframe selection across diverse video types. For implementation details, please refer to Algorithm 1. Since the outer while loop typically executes only a few times in practice, the overall complexity is approximately $\mathcal{O}(\max(|\mathcal{K}||\mathcal{C}|, |\mathcal{C}|\log|\mathcal{C}|))$, making the approach suitable for practical use. With the final keyframe set \mathcal{K} determined by our EFS, it is concatenated with the query Q and provided as input to a pre-trained LVLm. The model subsequently generates a comprehensive response: $\mathcal{R} = \text{LVLm}(\mathcal{K}, Q)$.

4. Experiments

4.1. Experimental Settings

Evaluation Benchmarks and Models. We evaluate our method on three long-video QA benchmarks: 1) VideoMME [9], consisting of 2,700 human-annotated QA pairs, with an average video duration of 17 minutes; 2) LongVideoBench [37], using the validation set containing 1,337 QA pairs, with an average video length of 12 minutes; 3) MLVU [45], a multi-task benchmark where we focus on the multiple-choice (M-avg) task, comprising 2,174 questions spanning 7 categories and an average duration of 11 minutes per video. To fairly assess the contribution of

keyframe selection, we do not leverage video subtitles in any experiments. We adopt three Large Vision-Language Models (LVLms) as baselines: LLaVA-OneVision [11], Qwen2.5-VL [2], and LLaVA-Video [44], all in their 7B variants. For fair comparison, we replicate all model results under a unified experimental setup.

Implementation Details. To reduce computational costs, candidate frames are uniformly sampled from each video at 1 frame per second. Query-to-frame matching scores are computed using the BLIP2-ITM-ViT-g model [12], while DINOv2 [27] is used for visual feature extraction. For all tasks, we report accuracy measured by the LMMs-Eval toolkit [41]. All experiments were conducted on an NVIDIA A800 GPU with 80 GB of memory.

4.2. Comparisons with State-of-the-Arts.

Comparisons with different LVLms. We first compare our method’s video question answering accuracy with leading LVLms, including proprietary models such as GPT-4o and open-source models like NVILA. These models differ in parameter scale, input frame capacity, and architecture, providing a broad evaluation of our method’s generalizability. As shown in Table 1, our Event-Anchored Frame Selection (EFS) consistently and substantially improves accuracy across all models and benchmarks. For example, when applied to LLaVA-OneVision (8 input frames), EFS boosts accuracy by 3.3% on VideoMME, 6.2% on LongVideoBench, and 8.8% on MLVU. For Qwen2.5-VL

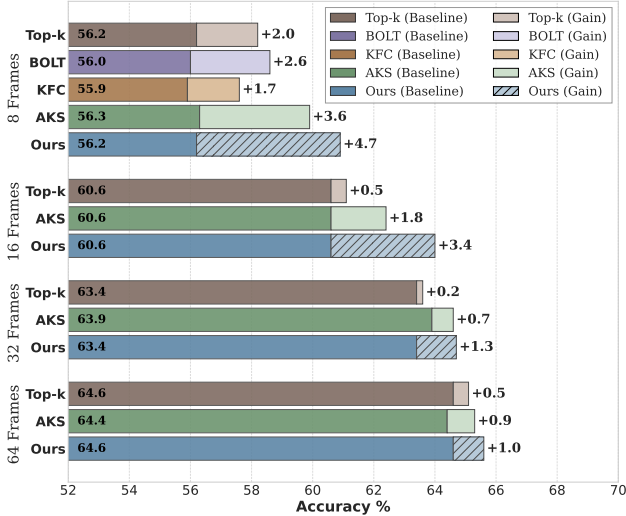
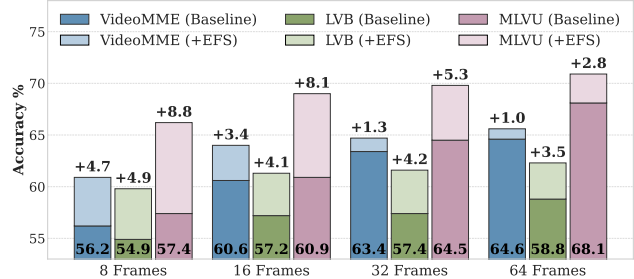


Figure 3. A quantitative comparison on VideoMME using LLaVA-Video-7B, where EFS consistently delivers the largest accuracy gains across 8/16/32/64-frame budgets over different sampling strategies. The text to the left of each bar represents the baseline performance for that method, while the text on the right indicates the corresponding gain.

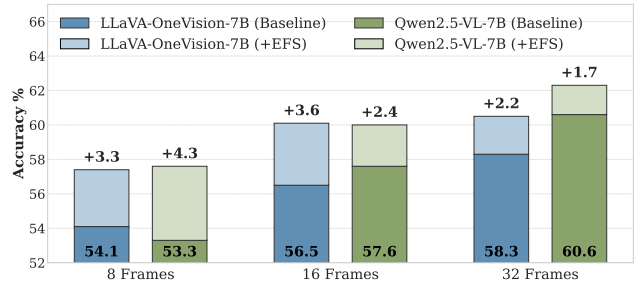
(16 frames), gains are 2.4%, 3.5%, and 9.5%, respectively. Even with the strongest baseline, LLaVA-Video (64 frames), EFS achieves improvements of 1.0%, 3.3%, and 2.8%. These enhancements allow smaller 7B-parameter models to outperform competing methods with similar computational budgets, and in some cases, even rival much larger models. For instance, LLaVA-Video-7B with EFS attains 65.6% accuracy on VideoMME, surpassing GPT-4o-mini by 0.8%. Similarly, LLaVA-OneVision with only 8 frames outperforms GPT-4o by 2.8% on MLVU with EFS, a result not possible with uniform frame selection. These findings underscore both the robust generalizability and the simple, plug-and-play benefits of EFS across a variety of models and input configurations.

Comparisons with different frame sampling strategies.

We further conduct a head-to-head comparison with recent query-based frame sampling methods, including Top-K, BOLT [17], KFC [8], and AKS [35]. All approaches are evaluated on VideoMME using LLaVA-Video-7B as the backbone, with improvements reported over a uniform sampling baseline for different numbers of input frames. As shown in Figure 3, EFS delivers the largest accuracy gains across all frame counts, outperforming baselines by 4.7%, 3.4%, 1.3%, and 1.0% at 8, 16, 32, and 64 frames, respectively. The Top-K approach provides minimal gains due to redundant selection. Although strategies like BOLT, KFC, and AKS seek to increase query relevance and frame diversity, their flat sampling paradigm often neglects the video’s intrinsic event structure. In summary, EFS consistently



(a) Performance of LLaVA-Video-7B Across Different Benchmarks



(b) Performance of Different Models on VideoMME

Figure 4. Video-based question answering accuracy (%) with different numbers of input frames.

achieves the most robust improvements, underscoring its effectiveness in informative frame selection and its advantage for accurate long-video understanding.

4.3. Ablation and Analysis

Various number of keyframes. To assess the generalizability of EFS, we evaluate its performance across varying frame budgets and multiple LVLMs, as illustrated in the Figure 4. On LLaVA-Video-7B (subplot a), EFS consistently outperforms uniform sampling on all three benchmarks, with especially large gains under tight budgets: using only 8 frames, accuracy improves by +4.7% on VideoMME, +4.9% on LongVideoBench, and +8.8% on MLVU; even at 64 frames—where the uniform baseline is stronger—EFS maintains clear advantages. Demonstrating model-agnostic behavior (subplot b), EFS likewise benefits LLaVA-OneVision-7B and Qwen2.5-VL-7B on VideoMME, yielding +3.3% and +4.3% improvements, respectively, with 8 frames. Collectively, these results indicate that EFS is a robust, plug-and-play module that delivers substantial accuracy gains irrespective of LVLm architecture or frame budget, underscoring its practical value in diverse settings.

Ablation on EFS Strategies. To validate the EFS pipeline, we conducted a component-wise ablation on LLaVA-Video-7B using 16 input frames (see Table 2 and Table 3).

1) Event Partitioning. In Table 2, defining event boundaries at local minima of the DINOv2 similarity curve achieves the best results, outperforming both random and

Table 2. Video-based question answering accuracy (%) of different Strategies in EFS. We compare the performance of our final method against variants with different strategies for event partitioning, anchor initialization, and the refinement process on the VideoMME and LVB benchmarks.

| Methods | | VideoMME | LVB |
|----------------------------|------------|-------------|-------------|
| Uniform Sampling | | 60.6 | 57.2 |
| Random Partition | | 62.9 | 59.8 |
| Clustered Partition | | 63.3 | 60.7 |
| Random Initialization | | 62.1 | 60.3 |
| Centralized Initialization | | 61.9 | 60.1 |
| MMR w.o. Adaptive | $\tau=0.4$ | 63.7 | 59.9 |
| | $\tau=0.6$ | 63.4 | 61.2 |
| | $\tau=0.8$ | 63.6 | 60.9 |
| Ours Method | | 64.0 | 61.3 |

Table 3. Video-based question answering accuracy (%) using different shot boundary detectors on LLaVA-Video-7B.

| Method | VideoMME | LVB |
|-------------------------|-------------|-------------|
| Uniform | 60.0 | 57.2 |
| Adaptive Detectors [4] | 63.6 | 60.3 |
| Content Detectors [4] | 63.6 | 60.4 |
| Hash Detectors [4] | 62.8 | 60.4 |
| Histogram Detectors [4] | 62.7 | 60.3 |
| Threshold Detectors [4] | 63.2 | 59.8 |
| Ours (DINOv2-based) | 64.0 | 61.3 |

clustered partitioning. This indicates that detecting natural temporal boundaries is more effective and computationally efficient than arbitrary or clustering-based divisions. Furthermore, to clarify the relationship between our method and traditional shot boundary detection, we conducted an additional experiment (Table 3). We substituted our DINOv2-based partitioning module with several established detectors from the PySceneDetect [4], which operate on lower-level visual cues. Our approach again outperforms all, supporting our hypothesis: although conceptually related to shot detection, exploiting powerful self-supervised features such as DINOv2 yields a more semantically faithful and accurate partitioning of video events—capabilities that are crucial for downstream reasoning tasks.

2) Anchor Initialization. Next, we examine how the initial anchor frames are selected within each event. Choosing the most query-relevant frame per event clearly surpasses both random or visual centroid-based selection, confirming that semantic relevance outweighs visual representativeness for video QA. Prioritizing query relevance enables the set of anchors is strongly aligned with user intent.

3) Adaptive Refinement. Finally, we validate our

Table 4. Ablation of signal acquisition. Left of “+” denotes the visual feature extractor for event detection, while the right side is the model for query-frame relevance scoring.

| Methods | Frames | VideoMME | LVB |
|--------------------|--------|------------------|------------------|
| Uniform | 8/16 | 56.2/60.6 | 54.9/57.2 |
| CLIP + CLIP | 8/16 | 60.2/63.1 | 57.6/60.2 |
| DINOv2 + CLIP | 8/16 | 60.5/63.1 | 58.4/60.3 |
| CLIP + BLIP2-ITM | 8/16 | 60.4/63.3 | 58.8/60.4 |
| DINOv2 + BLIP2-ITM | 8/16 | 60.9/64.0 | 59.8/61.3 |

Table 5. Ablation study on the hyper-parameters M (maximum number of events) and α (threshold relaxation factor). All experiments are conducted on the VideoMME using LLaVA-Video-7B.

| $M \backslash \alpha$ | 0.1 | 0.3 | 0.4 | 0.5 | 0.6 | 0.7 | 0.9 |
|-----------------------|------|------|------|-------------|------|------|------|
| 1 | 61.4 | 61.3 | 61.0 | 61.5 | 61.7 | 61.9 | 61.6 |
| 4 | 62.5 | 62.4 | 62.4 | 62.5 | 62.2 | 61.9 | 61.4 |
| 8 | 62.6 | 62.9 | 62.8 | 62.7 | 62.4 | 62.6 | 62.2 |
| 10 | 63.0 | 63.4 | 63.8 | 64.0 | 63.6 | 63.4 | 63.5 |
| 12 | 63.0 | 63.1 | 63.1 | 63.3 | 62.9 | 63.4 | 63.4 |
| 14 | 63.4 | 63.2 | 63.3 | 63.4 | 62.9 | 63.2 | 62.7 |
| 16 | 63.1 | 63.0 | 63.1 | 63.2 | 63.0 | 63.2 | 63.0 |

adaptive refinement mechanism. As shown in Table 2, Our anchor-guided adaptive refinement consistently outperforms a standard MMR implementation with a fixed diversity threshold τ , as no static threshold generalizes across both benchmarks. Dynamically adjusting the diversity criteria based on each video’s unique content yields the top results (64.0/61.3%), demonstrating the robustness and effectiveness of content-adaptive refinement.

Visual and semantic signal Ablations. We further ablate the signal acquisition components of our framework (Table 4). For event boundary detection, DINOv2 consistently outperforms CLIP [30], likely due to its superior capture of fine-grained visual changes, providing a more accurate representation of visual events than the high-level semantic features of CLIP. For relevance scoring, BLIP2-ITM shows clear gains over CLIP, highlighting the benefit of dedicated image-text matching. Combining DINOv2 for event structure with BLIP2-ITM for relevance delivers the best performance, supporting our design choices.

Hyper-parameter Ablation. We investigate two critical hyper-parameters, the maximum event number M and the relaxation factor α , with a comprehensive grid search summarized in Table 5. M controls the video partition granularity. Performance peaks at $M=10$, as smaller values lead to coarse, under-segmented events, while larger values cause over-partitioning and noisy anchors. Concurrently, α governs the diversity threshold in our adaptive MMR. The re-

sults show that an intermediate value of $\alpha=0.5$ is optimal, as it balances capturing intrinsic visual variance without being overly restrictive and filtering out relevant frames. This optimal configuration ($M=10, \alpha=0.5$) achieves a state-of-the-art accuracy of 64.0% on VideoMME.

Table 6. Computational cost and accuracy comparison on VideoMME with LLaVA-Video-7B. We report average per-video time (seconds) for each component. All experiments conducted on a single NVIDIA A800 GPU with two Intel Xeon Silver 4314 CPUs (16 cores), at 1 fps with 16 input frames.

| Component | Short | Medium | Long | Overall |
|--------------------------------------|--------------|--------------|--------------|--------------|
| <i>Preprocessing Time (seconds):</i> | | | | |
| Video Reading | 1.45 | 9.40 | 48.94 | 19.93 |
| Vision Signal | 1.16 | 7.45 | 33.75 | 14.12 |
| Semantic Signal | 1.34 | 8.48 | 40.75 | 16.85 |
| EFS Selection | 0.03 | 0.16 | 0.95 | 0.38 |
| Total Preprocess (s) | 4.0 | 25.5 | 124.4 | 51.3 |
| LVLm Inference (s) | 2.39 | 2.99 | 3.51 | 2.97 |
| Accuracy (%) | 76.33 | 62.67 | 53.00 | 64.00 |
| vs. Uniform | +4.22 | +4.34 | +1.78 | +3.44 |

Efficiency and Cost-Effectiveness Analysis. To contextualize our method’s efficiency, we report its computational overhead in Table 6. Although EFS introduces a preprocessing cost absent in uniform sampling, this overhead is justified by a considerable +3.44% gain in overall accuracy. The analysis reveals that the primary computational bottlenecks are the vision and semantic signal extraction steps, while the EFS selection stage itself is remarkably lightweight, consuming less than 1% of the total preprocessing time. This demonstrates that the core logic of our method is highly efficient. This trade-off—investing moderate computational resources for a significant accuracy improvement—renders EFS a practical and cost-effective choice for applications where performance is paramount and offline processing is feasible, such as in-depth content analysis. Furthermore, this overhead is not static; it can be substantially reduced. The feature extraction bottleneck can be accelerated through future optimizations like model quantization and hardware-specific enhancements. Moreover, for long videos where the cost is highest, performance can be maintained while significantly reducing processing time by moderately lowering the input frame-per-second.

4.4. Visualization

Figure 5 presents two qualitative examples from VideoMME that illustrate the advantages of our Event-Anchored Frame Selection (EFS) over uniform sampling. In both video QA cases—a bottle DIY and a crafting tutorial—the uniform baseline, being temporally agnostic, misses key events and yields incorrect answers. By con-

trast, EFS leverages Image-Text Matching (ITM) scores and inter-frame similarity to uncover the underlying event structure of the video content and then strategically selects frames to ensure comprehensive event coverage. As a result, the LVLm receives the necessary evidence for accurate reasoning and correct responses.

5. Conclusion

In this paper, we introduce Event-Anchored Frame Selection (EFS), a training-free frame selection method designed to boost LVLms for long-form video understanding. By leveraging intrinsic event structure of the video, EFS constructs a keyframe representation optimized for event coverage, query relevance, and visual diversity. This event-aware approach yields significant gains across major benchmarks, confirming its superiority over flat, temporally-agnostic sampling for effective long-video reasoning. Further discussion and additional experiments are provided in the Appendix.

References

- [1] Josh Achiam, Steven Adler, Sandhini Agarwal, Lama Ahmad, Ilge Akkaya, Florencia Leoni Aleman, Diogo Almeida, Janko Altschmidt, Sam Altman, Shyamal Anadkat, et al. Gpt-4 technical report. *arXiv preprint arXiv:2303.08774*, 2023. 1
- [2] Shuai Bai, Keqin Chen, Xuejing Liu, Jialin Wang, Wenbin Ge, Sibao Song, Kai Dang, Peng Wang, Shijie Wang, Jun Tang, et al. Qwen2. 5-vl technical report. *arXiv preprint arXiv:2502.13923*, 2025. 5
- [3] Jaime Carbonell and Jade Goldstein. The use of mmr, diversity-based reranking for reordering documents and producing summaries. In *ACM SIGIR*, pages 335–336, 1998. 4
- [4] Brandon Castellano. Pyscenedetect. <https://www.scenedetect.com/>, 2025. Version 0.6.7; Online; accessed 2025-08-24. 7
- [5] Lin Chen, Xilin Wei, Jinsong Li, Xiaoyi Dong, Pan Zhang, Yuhang Zang, Zehui Chen, Haodong Duan, Zhenyu Tang, Li Yuan, et al. Sharegpt4video: Improving video understanding and generation with better captions. In *NeurIPS*, pages 19472–19495, 2024. 1
- [6] Chuanqi Cheng, Jian Guan, Wei Wu, and Rui Yan. Scaling video-language models to 10k frames via hierarchical differential distillation. *arXiv preprint arXiv:2504.02438*, 2025. 4
- [7] Yue Fan, Xiaojian Ma, Rujie Wu, Yuntao Du, Jiaqi Li, Zhi Gao, and Qing Li. Videoagent: A memory-augmented multimodal agent for video understanding. In *ECCV*, pages 75–92. Springer, 2024. 2
- [8] Bo Fang, Wenhao Wu, Qiangqiang Wu, Yuxin Song, and Antoni B Chan. Threading keyframe with narratives: Mllms as strong long video comprehenders. *arXiv preprint arXiv:2505.24158*, 2025. 2, 6

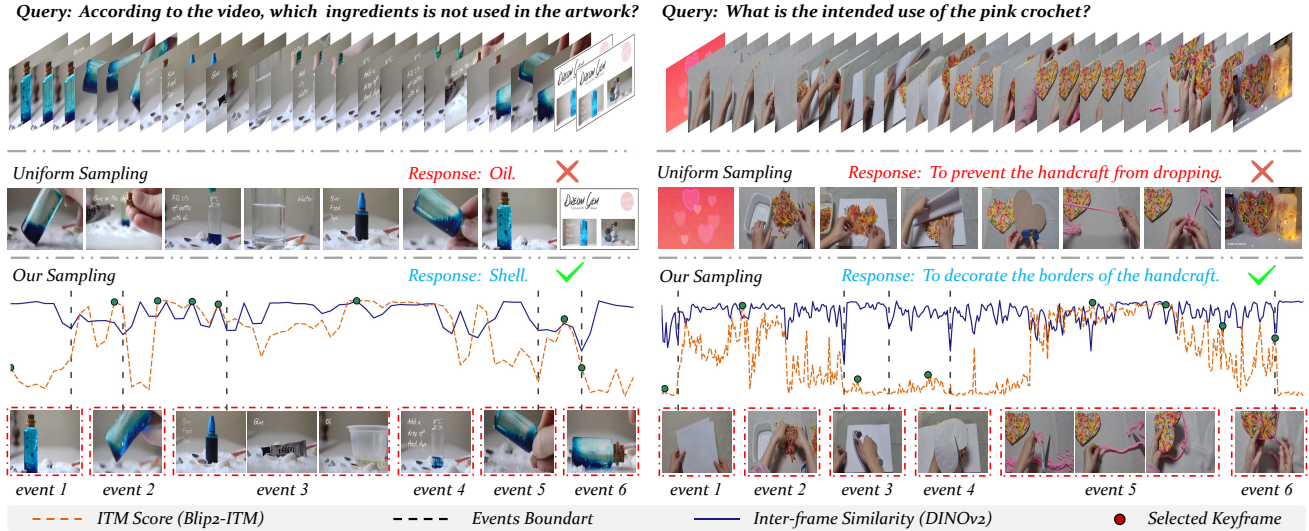


Figure 5. Qualitative comparison of our EFS versus the uniform sampling. The uniform baseline fails by missing key events, while EFS explicitly identifies the video’s underlying event structure, enabling accurate reasoning and correct answers. Please zoom in for details.

[9] Chaoyou Fu, Yuhan Dai, Yongdong Luo, Lei Li, Shuhuai Ren, Renrui Zhang, Zihan Wang, Chenyu Zhou, Yunhang Shen, Mengdan Zhang, et al. Video-mme: The first-ever comprehensive evaluation benchmark of multi-modal llms in video analysis. In *CVPR*, pages 24108–24118, 2025. 2, 5

[10] De-An Huang, Subhashree Radhakrishnan, Zhiding Yu, and Jan Kautz. Frag: Frame selection augmented generation for long video and long document understanding. *arXiv preprint arXiv:2504.17447*, 2025. 2

[11] Bo Li, Yuanhan Zhang, Dong Guo, Renrui Zhang, Feng Li, Hao Zhang, Kaichen Zhang, Peiyuan Zhang, Yanwei Li, Ziwei Liu, et al. Llava-onevision: Easy visual task transfer. *arXiv preprint arXiv:2408.03326*, 2024. 5

[12] Junnan Li, Dongxu Li, Silvio Savarese, and Steven Hoi. Blip-2: Bootstrapping language-image pre-training with frozen image encoders and large language models. In *ICML*, pages 19730–19742. PMLR, 2023. 3, 5, 1

[13] Yanwei Li, Chengyao Wang, and Jiaya Jia. Llama-vid: An image is worth 2 tokens in large language models. In *ECCV*, pages 323–340. Springer, 2024. 2

[14] Bin Lin, Yang Ye, Bin Zhu, Jiayi Cui, Munan Ning, Peng Jin, and Li Yuan. Video-llava: Learning united visual representation by alignment before projection. In *EMNLP*, pages 5971–5984, 2024. 2, 5

[15] Haotian Liu, Chunyuan Li, Qingyang Wu, and Yong Jae Lee. Visual instruction tuning. In *NeurIPS*, pages 34892–34916, 2023. 1

[16] Hao Liu, Wilson Yan, Matei Zaharia, and Pieter Abbeel. World model on million-length video and language with blockwise ringattention. *arXiv preprint arXiv:2402.08268*, 2024. 1, 2

[17] Shuming Liu, Chen Zhao, Tianqi Xu, and Bernard Ghanem. Bolt: Boost large vision-language model without training for long-form video understanding. In *CVPR*, pages 3318–3327, 2025. 2, 6

[18] Zhijian Liu, Ligeng Zhu, Baifeng Shi, Zhuoyang Zhang, Yuming Lou, Shang Yang, Haocheng Xi, Shiyi Cao, Yuxian Gu, Dacheng Li, et al. Nvlla: Efficient frontier visual language models. In *CVPR*, pages 4122–4134, 2025. 5

[19] Yongdong Luo, Xiawu Zheng, Xiao Yang, Guilin Li, Haojia Lin, Jinfa Huang, Jiayi Ji, Fei Chao, Jiebo Luo, and Rongrong Ji. Video-rag: Visually-aligned retrieval-augmented long video comprehension. *arXiv preprint arXiv:2411.13093*, 2024. 2

[20] Yongdong Luo, Wang Chen, Xiawu Zheng, Weizhong Huang, Shukang Yin, Haojia Lin, Chaoyou Fu, Jinfa Huang, Jiayi Ji, Jiebo Luo, et al. Quota: Query-oriented token assignment via cot query decouple for long video comprehension. *arXiv preprint arXiv:2503.08689*, 2025. 2

[21] Ziyu Ma, Chenhui Gou, Hengcan Shi, Bin Sun, Shutao Li, Hamid Rezaatofghi, and Jianfei Cai. Drvideo: Document retrieval based long video understanding. In *CVPR*, pages 18936–18946, 2025. 1, 2

[22] Muhammad Maaz, Hanoona Rasheed, Salman Khan, and Fahad Khan. Video-chatgpt: Towards detailed video understanding via large vision and language models. In *ACL*, pages 12585–12602, 2024. 2

[23] Juhong Min, Shyamal Buch, Arsha Nagrani, Minsu Cho, and Cordelia Schmid. Morevqa: Exploring modular reasoning models for video question answering. In *CVPR*, pages 13235–13245, 2024. 1

[24] Azra Nasreen and G Dr Shobha. Key frame extraction using edge change ratio for shot segmentation. *IJARCCCE*, 2(11): 4421–4423, 2013. 2

[25] OpenAI. Gpt-4o mini:advancing cost-efficient intelligence. <https://openai.com/index/gpt-4o-mini-advancing-cost-efficient-intelligence/>, 2024. Accessed: 2024-06-18. 5

[26] OpenAI. Hello gpt-4o. <https://openai.com/>

- [index/hello-gpt-4o/](#), 2024. Accessed: 2024-05-13. 5
- [27] Maxime Oquab, Timothée Darcet, Théo Moutakanni, Huy Vo, Marc Szafraniec, Vasil Khalidov, Pierre Fernandez, Daniel Haziza, Francisco Massa, Alaaeldin El-Nouby, et al. Dinov2: Learning robust visual features without supervision. *arXiv preprint arXiv:2304.07193*, 2023. 3, 5, 1
- [28] Jongwoo Park, Kanchana Ranasinghe, Kumara Kahatapitiya, Wonjeong Ryu, Donghyun Kim, and Michael S Ryoo. Too many frames, not all useful: Efficient strategies for long-form video qa. *arXiv preprint arXiv:2406.09396*, 2024. 2
- [29] Long Qian, Juncheng Li, Yu Wu, Yaobo Ye, Hao Fei, Tat-Seng Chua, Yueting Zhuang, and Siliang Tang. Momen-tor: advancing video large language model with fine-grained temporal reasoning. In *ICML*, pages 41340–41356, 2024. 1
- [30] Alec Radford, Jong Wook Kim, Chris Hallacy, Aditya Ramesh, Gabriel Goh, Sandhini Agarwal, Girish Sastry, Amanda Askell, Pamela Mishkin, Jack Clark, et al. Learning transferable visual models from natural language super-vision. In *ICML*, pages 8748–8763. PmLR, 2021. 7
- [31] C Va Sheena and NK Narayanan. Key-frame extraction by analysis of histograms of video frames using statistical meth-ods. *Procedia Computer Science*, 70:36–40, 2015. 2
- [32] Xiaoqian Shen, Yunyang Xiong, Changsheng Zhao, Lemeng Wu, Jun Chen, Chenchen Zhu, Zechun Liu, Fanyi Xiao, Bal-akrishnan Varadarajan, Florian Bordes, et al. Longvu: Spa-tiotemporal adaptive compression for long video-language understanding. *arXiv preprint arXiv:2410.17434*, 2024. 2, 5
- [33] Yan Shu, Zheng Liu, Peitian Zhang, Minghao Qin, Jun-jie Zhou, Zhengyang Liang, Tiejun Huang, and Bo Zhao. Video-xl: Extra-long vision language model for hour-scale video understanding. In *CVPR*, pages 26160–26169, 2025. 5
- [34] Hui Sun, Shiyin Lu, Huanyu Wang, Qing-Guo Chen, Zhao Xu, Weihua Luo, Kaifu Zhang, and Ming Li. Mdp3: A training-free approach for list-wise frame selection in video-llms. *arXiv preprint arXiv:2501.02885*, 2025. 2
- [35] Xi Tang, Jihao Qiu, Lingxi Xie, Yunjie Tian, Jianbin Jiao, and Qixiang Ye. Adaptive keyframe sampling for long video understanding. In *CVPR*, pages 29118–29128, 2025. 2, 6
- [36] Peng Wang, Shuai Bai, Sinan Tan, Shijie Wang, Zhihao Fan, Jinze Bai, Keqin Chen, Xuejing Liu, Jialin Wang, Wenbin Ge, et al. Qwen2-vl: Enhancing vision-language model’s perception of the world at any resolution. *arXiv preprint arXiv:2409.12191*, 2024. 1
- [37] Haoning Wu, Dongxu Li, Bei Chen, and Junnan Li. Longvideobench: A benchmark for long-context interleaved video-language understanding. In *NeurIPS*, pages 28828–28857, 2024. 2, 5
- [38] Zeyu Xu, Junkang Zhang, Qiang Wang, and Yi Liu. E-vrag: Enhancing long video understanding with resource-efficient retrieval augmented generation. *arXiv preprint arXiv:2508.01546*, 2025. 2
- [39] Jinhui Ye, Zihan Wang, Haosen Sun, Keshigeyan Chan-drasegaran, Zane Durante, Cristobal Eyzaguirre, Yonatan Bisk, Juan Carlos Niebles, Ehsan Adeli, Li Fei-Fei, et al. Re-thinking temporal search for long-form video understanding. In *CVPR*, pages 8579–8591, 2025. 2
- [40] Sicheng Yu, Chengkai Jin, Huanyu Wang, Zhenghao Chen, Sheng Jin, Zhongrong Zuo, Xiaolei Xu, Zhenbang Sun, Bingni Zhang, Jiawei Wu, et al. Frame-voyager: Learn-ing to query frames for video large language models. *arXiv preprint arXiv:2410.03226*, 2024. 2, 5
- [41] Kaichen Zhang, Bo Li, Peiyuan Zhang, Fanyi Pu, Joshua Adrian Cahyono, Kairui Hu, Shuai Liu, Yuanhan Zhang, Jingkang Yang, Chunyuan Li, et al. Lmms-eval: Re-ality check on the evaluation of large multimodal models. In *NAACL*, pages 881–916, 2025. 5
- [42] Peiyuan Zhang, Kaichen Zhang, Bo Li, Guangtao Zeng, Jingkang Yang, Yuanhan Zhang, Ziyue Wang, Haoran Tan, Chunyuan Li, and Ziwei Liu. Long context transfer from language to vision. *arXiv preprint arXiv:2406.16852*, 2024. 1, 2, 5
- [43] Shaojie Zhang, Jiahui Yang, Jianqin Yin, Zhenbo Luo, and Jian Luan. Q-frame: Query-aware frame selection and multi-resolution adaptation for video-llms. *arXiv preprint arXiv:2506.22139*, 2025. 2
- [44] Yuanhan Zhang, Jinming Wu, Wei Li, Bo Li, Zejun Ma, Zi-wei Liu, and Chunyuan Li. Video instruction tuning with synthetic data. *arXiv preprint arXiv:2410.02713*, 2024. 5
- [45] Junjie Zhou, Yan Shu, Bo Zhao, Boya Wu, Shitao Xiao, Xi Yang, Yongping Xiong, Bo Zhang, Tiejun Huang, and Zheng Liu. Mlvu: A comprehensive benchmark for multi-task long video understanding. *arXiv preprint arXiv:2406.04264*, 2024. 2, 5

Event-Anchored Frame Selection for Effective Long-Video Understanding

Supplementary Material

6. Limitations and Future Work

6.1. Limitations

Despite its demonstrated efficacy, our Event-Anchored Frame Selection (EFS) framework is subject to several inherent limitations that warrant discussion.

- **Preprocessing Overhead.** Preprocessing Overhead. Our pipeline requires an offline signal extraction stage based on pretrained DINOv2 [27] and BLIP2-ITM [12], incurring computational costs that uniform sampling avoids. For long videos, generating these signals constitutes a substantial preprocessing burden, which can render EFS impractical in latency-sensitive or real-time settings.
- **Heuristic and Hyperparameter Sensitivity.** EFS is a multi-stage, heuristic-driven pipeline whose performance hinges on several key hyperparameters, most notably the number of events M and the relaxation factor (α). Although we identify workable configurations via grid search, these settings may not transfer across video domains or downstream tasks. The current framework lacks a principled, data-driven procedure for automatic hyperparameter adaptation, leaving performance sensitive to manual choices.
- **Dependence on Upstream Models.** The performance of EFS is intrinsically coupled with the representational power of the foundational DINOv2 and BLIP2-ITM models. Consequently, EFS inherits not only their capabilities but also their limitations. Any inherent biases, domain gaps, or catastrophic failures within these upstream models can propagate downstream, adversely affecting the quality of the final frame selection.

6.2. Future Works

The limitations of our current approach highlight several promising directions for future research.

- **System-Level Efficiency Enhancement.** A primary objective is to reduce the end-to-end latency of the proposed framework. Future work will focus on holistic system-level optimizations across the entire pipeline. This includes accelerating data ingestion and processing, designing more efficient computational pathways, and exploring hardware-aware execution strategies to ensure stable, low-latency performance under strict resource constraints without compromising selection quality.
- **Omni-Modal Event Understanding.** To achieve a more robust and context-aware analysis, we plan to move beyond purely visual cues and develop an omni-modal framework. This involves integrating diverse data streams—such as high-level semantics, motion dynamics,

audio signals, and textual transcriptions—into a unified representation. By fusing these multimodal signals, the model can learn to identify complex event boundaries and resolve ambiguities that are imperceptible from visual information alone, leading to a more holistic understanding of the video content.

- **End-to-End Trainable Selection.** A key ambition is to replace the current heuristic-based pipeline with a fully end-to-end trainable model. This would involve designing a differentiable selection module that learns to identify key content by directly optimizing for the downstream task objective. Such a data-driven approach would not only eliminate the need for manual hyperparameter tuning but also has the potential to discover more effective and adaptive selection strategies than a handcrafted pipeline, ultimately yielding a more powerful and generalizable solution.

7. More Experimental Results

7.1. Comparisons with Different Subtasks in VideoMME

For a fine-grained evaluation of our Event-Anchored Frame Selection (EFS) method, we conducted a comprehensive comparative analysis against a uniform sampling baseline on the VideoMME benchmark. Both methods were evaluated using the LLaVA-Video-7B model, with the input constrained to eight frames. This setup allowed for a detailed assessment of performance across all 12 subtasks, revealing the specific domains where EFS provides the most significant advantages.

As illustrated in Figure 6, EFS demonstrates superior performance to the baseline across every subtask, underscoring its broad-spectrum efficacy rather than a narrow, task-specific benefit. The most substantial gains are observed in tasks demanding high perceptual acuity and temporal awareness, including Spatial Perception (+11.11%), Temporal Perception (+9.09%), and OCR Problems (+7.91%). This highlights EFS’s strength in capturing and preserving essential scene context, sequential order, and fine-grained visual details. Moreover, notable improvements in complex, high-level tasks such as Spatial Reasoning (+5.35%), Action Reasoning (+4.92%), and Temporal Reasoning (+4.52%) further affirm the generalizability of our approach. The consistent performance uplift across this diverse range of tasks, from low-level perception to advanced reasoning, validates EFS as a robust and effective framework for long-video understanding, particularly under the practical limitation of a finite context window.

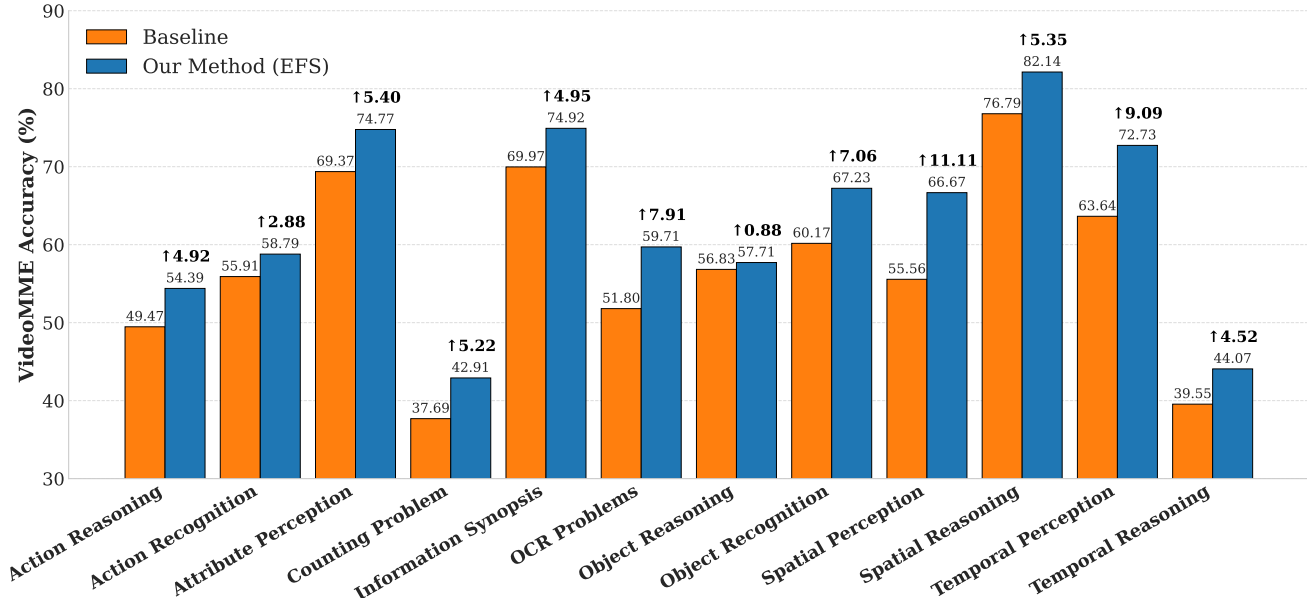


Figure 6. Detailed performance comparison of our method (EFS) against the baseline across all 12 subtasks of the Video-MME benchmark [9]. The results demonstrate that our EFS approach consistently surpasses the baseline in every category, underscoring the broad effectiveness of our method in enhancing diverse video understanding capabilities.

Table 7. Ablation on the window size l . We report the video-based question answering accuracy (%) on the VideoMME, LVB, and MLVU benchmarks. The best results are highlighted in **bold**.

| Method | VideoMME | LVB(val) | MLVU |
|------------------------------|-------------|-------------|-------------|
| <i>uniform</i> | 60.6 | 57.2 | 60.9 |
| <i>EFS($l=3$)</i> | 64.0 | 61.3 | 69.0 |
| <i>EFS($l=5$)</i> | 63.3 | 61.7 | 68.0 |
| <i>EFS($l=7$)</i> | 63.4 | 60.9 | 68.6 |

7.2. Ablation Study on Window Size

The window size, denoted as l , is a critical hyperparameter in our Event-Anchored Frame Selection (EFS) framework, as it defines the temporal scope for computing inter-frame similarity. The choice of l involves a direct trade-off: a smaller window enhances sensitivity to rapid, fine-grained scene changes, while a larger one provides a more robust measure of local temporal coherence. To systematically investigate this trade-off and determine an optimal configuration, we conducted an ablation study with l set to 3, 5, and 7. The performance of each variant was evaluated against a uniform sampling baseline across three diverse video understanding benchmarks: VideoMME [9], LongVideoBench (LVB)[37], and MLVU[45].

As summarized in Table 7, all configurations of EFS substantially outperform the uniform sampling baseline, affirming the fundamental advantage of content-aware selection.

Among the tested variants, a window size of $l=3$ yields the strongest overall performance, achieving state-of-the-art results of 64.0% on VideoMME and 69.0% on MLVU. Although the $l=5$ setting shows a marginal advantage on the LVB validation set, its performance on the other benchmarks declines. Increasing the window to $l=7$ leads to a more pronounced degradation in accuracy. These results strongly indicate that a compact window ($l=3$) is most effective at capturing the salient, short-term visual dynamics crucial for downstream comprehension tasks. In contrast, larger windows risk over-smoothing the temporal signal, thereby obscuring important transitional moments. Consequently, we adopt $l=3$ as the default window size for our EFS framework in all subsequent experiments.

7.3. Hyperparameter Ablation Study

To dissect the contributions of our framework’s key components, we conduct a comprehensive ablation study on two critical hyperparameters: the maximum number of video events, M , and the threshold relaxation factor, α , used in our adaptive MMR algorithm. We perform a grid search on these parameters and report the accuracy on the VideoMME, LongVideoBench (LVB), and MLVU benchmarks.

Impact of Event Granularity (M). The hyperparameter M dictates the granularity of the initial video partition. An optimal value for M must strike a balance: if M is too small, distinct semantic events may be merged, leading to a coarse-grained perception and a poor set of initial anchors.

Conversely, if M is excessively large, a single event might be over-partitioned, introducing noisy or redundant anchors that undermine the subsequent refinement process.

As shown in Table 5, our empirical results on VideoMME corroborate this trade-off. Performance steadily improves as M increases from 1 to 10, peaking at an accuracy of **64.0%**. However, further increasing M to 12 and beyond leads to a marginal but consistent decline in performance. A similar trend is observed on the LongVideoBench and MLVU datasets (Table 8), where the performance peaks when M is in the range of 12 to 14. This consistent pattern across benchmarks validates our hypothesis that an intermediate event granularity is crucial for building a representative and effective structural prior for frame selection.

Impact of Threshold Relaxation Factor (α). The relaxation factor, α , controls the flexibility of the diversity thresholds in our adaptive MMR framework. A small α enforces a narrow and rigid diversity range, which may fail to adapt to the video’s intrinsic visual variance. In contrast, a large α makes the similarity threshold overly loose (or strict, depending on formulation), potentially filtering out relevant frames and thus reducing coverage.

Interestingly, the optimal value for α exhibits a dataset-specific nature. For VideoMME (Table 5), a moderate $\alpha=0.5$ achieves the best balance, enabling the model to dynamically adjust to the video’s statistical characteristics. However, for both LongVideoBench and MLVU (Table 8), a much smaller value of $\alpha=0.1$ consistently yields the best results. This suggests that the videos in LVB and MLVU may possess more uniform event structures or statistical properties, benefiting from a stricter and less adaptive diversity criterion. The optimal configuration for LVB is ($M=14, \alpha=0.1$), achieving **61.3%**, and for MLVU is ($M=14, \alpha=0.1$), achieving **69.0%**.

These findings underscore that while the general trends of our hyperparameters are consistent, their optimal values are influenced by the unique statistics and event structures of each dataset. This highlights the importance of data-aware priors in guiding the frame selection process effectively.

7.4. Generalizability to Information Synopsis Queries

Our EFS method is fundamentally query-based, which raises a question about its effectiveness on information synopsis queries (e.g., “What does this video describe?”). Intuitively, for such general questions where specific semantic signals are absent, the query-centric anchor selection of EFS might not be beneficial, and a simpler uniform sampling approach could suffice.

To investigate this, we conducted an experiment to determine if an LVLM could dynamically choose the appropri-

Table 8. Ablation of M and α . Results are shown as accuracy (%) on LongVideoBench/MLVU.

| $M \backslash \alpha$ | 0.1 | 0.3 | 0.5 | 0.7 |
|-----------------------|-------------------|-----------|-----------|-----------|
| 1 | 59.5/68.2 | 58.7/68.0 | 58.3/67.6 | 58.8/67.6 |
| 4 | 60.0/67.9 | 59.6/67.6 | 59.8/68.3 | 59.6/67.8 |
| 8 | 59.7/68.0 | 60.0/68.0 | 59.7/67.5 | 59.0/67.9 |
| 10 | 60.0/68.6 | 60.0/68.5 | 60.3/67.7 | 60.4/67.7 |
| 12 | 60.6/ 69.0 | 59.8/68.0 | 60.4/68.0 | 59.9/68.1 |
| 14 | 61.3/69.0 | 60.4/68.6 | 61.1/68.5 | 60.3/68.7 |
| 16 | 60.1/67.8 | 59.9/67.8 | 59.9/67.8 | 60.1/67.8 |

ate sampling strategy. We implemented a Chain-of-Thought (CoT) based router: for each query, the LLaVA-Video model was first prompted to classify the query as either specific and targeted, or general and synopsis-oriented. The exact prompt used for this classification is detailed in 7.5. If the model identified a query as specific, we applied our EFS method. If it deemed the query general, the system reverted to a standard uniform sampling strategy. We refer to this hybrid approach as “part EFS”. All experiments were conducted with a 16-frame input limit.

The results are presented in Table 9. Counter-intuitively, the adaptive “part EFS” strategy consistently underperformed the full EFS approach across all three benchmarks. For instance, on VideoMME, reverting to uniform sampling for general queries resulted in a 1.5% drop in accuracy compared to always using EFS. This performance degradation demonstrates that forcing a fallback to uniform sampling for general queries is a detrimental choice. The result strongly suggests that the structural priors and enhanced event coverage provided by EFS are beneficial even for information synopsis tasks, outperforming the temporally-agnostic nature of uniform sampling. This conclusion is further supported by the performance gains observed on the Information Synopsis sub-task, as illustrated in Figure 6.

Table 9. Performance comparison of the CoT-based adaptive sampling strategy. The performance drop in “part EFS” highlights the universal effectiveness of EFS, even on general queries where the system reverted to uniform sampling.

| Methods | VideoMME | LVB | MLVU |
|------------------------|------------|------------|------------|
| LLaVA-Video (Uniform) | 60.6 | 57.2 | 60.9 |
| LLaVA-Video + EFS | 64.0 | 61.3 | 69.0 |
| LLaVA-Video + part EFS | 62.5(-1.5) | 60.7(-0.6) | 68.6(-0.4) |

7.5. Additional Qualitative Examples

To further validate the rationality of our event partitioning, Figure 7 presents a t-SNE visualization of DINOv2 features extracted from sampled video frames. The clear clustering

and separation of points confirm that our method groups visually consistent events and identifies meaningful event boundaries. This establishes a reliable foundation for subsequent keyframe selection.

System Prompt: Video Query Classifier

You are an expert assistant in video analysis. Your task is to determine if a user’s question necessitates a query-based keyframe selection method. This method is designed for finding specific moments, objects, or actions within a video.

Analyze the user’s question. Think step-by-step to decide if it’s a specific query or a general one. After your reasoning, provide your final answer on a new line. The final answer must be ONLY ‘Yes’ or ‘No’. ‘Yes’ means the question requires a specific, targeted search. ‘No’ means the question is general, asking for a summary or an overall idea.

Example 1:

Question: “Summarize what this video is about.”

Reasoning: This is a high-level request for a general overview. It does not require locating a specific moment.

Final Answer: No

Example 2:

Question: “Find the scene where the cat knocks over the vase.”

Reasoning: This asks to locate a very specific action (“knocks over the vase”) involving specific subjects (“cat”, “vase”). This requires a targeted search.

Final Answer: Yes

Example 3:

Question: “What is the overall sentiment of the speaker?”

Reasoning: This question is about the general tone throughout the video, not a single instant. It is a holistic analysis.

Final Answer: No

Example 4:

Question: “When does the CEO appear on screen?”

Reasoning: This requires identifying all specific moments when a particular person (“the CEO”) is visible. This is a query-specific task.

Final Answer: Yes

Your Task:

Question: {Your Question}

Reasoning:

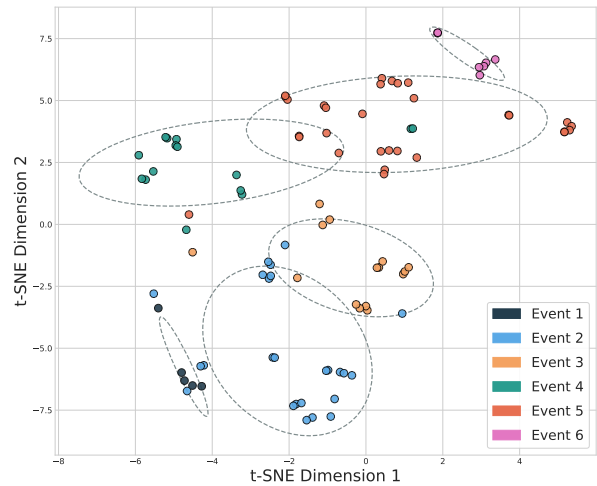


Figure 7. T-SNE visualization of DINOv2 features for sampled video frames. Each point represents one frame, and color indicates the event predicted by our EFS pipeline.